We are IntechOpen, the world's leading publisher of Open Access books Built by scientists, for scientists

4,800
Open access books available

122,000
International authors and editors

135M
Downloads

Our authors are among the

154
Countries delivered to

TOP 1%
most cited scientists

12.2%
Contributors from top 500 universities

CLARIVATE ANALYTICS BOOK CITATION INDEX INDEXED

WEB OF SCIENCE™

Selection of our books indexed in the Book Citation Index in Web of Science™ Core Collection (BKCI)

Interested in publishing with us?
Contact book.department@intechopen.com

Numbers displayed above are based on latest data collected.
For more information visit www.intechopen.com

13

Robust-Adaptive Flux Observers in Speed Vector Control of Induction Motor Drives

Filote Constantin[1,2] and Ciufudean Calin[1]
[1]*Stefan cel Mare University of Suceava*
[2]*SC Germaro Electronics SRL*
Romania

1. Introduction

The speed control of induction motors can be divided into two distinct strategies, depending on the type of dynamics that is required: scalar control (static control of the torque) and vector control (dynamic control of the torque) (Blaabjerg et al. 2005; Bose, 2000, 2006; Filote et al. 2009; Holtz, 2002; Leonhard, 1990; Umanand & Bhat, 1995; Vas, 1998).
Since the couple and flux levels depend on the motor behavior to frequency and voltage applied to it, maintaining the flux constant is strongly required in scalar control (V/f control). Despite the simplicity and the low cost implementation of the control method, it still presents the disadvantage of poor torque dynamics.
Vector control reassesses one of the advantages of direct current (dc) drives, which is the separation of speed and couple loops. According to its structure and to its own functioning principle, the dc drive is naturally field oriented, hence, the separation of the speed and current loops.
In the case of vector controllers of induction motor, the magnitude and phase stator current are controlled in accordance with the flux vector. There are three vector control strategies according to the type of drive-controlled flux: stator flux, rotor flux and air gap flux.
We can determine the magnitude and position of the rotor flux by using flux sensors (direct field-oriented control), estimators or observers (indirect field-oriented control) and by measuring some electrical and mechanical measurable states of electrical drives induction motor systems.
When the rotor flux estimation is performed after measuring only the electrical measurable states (voltages and stator currents), in this case we have a sensorless vector control system.
The implementation of the direct field-oriented control requires the measurement or calculation of the flux space vector (magnitude and position). The measurement of the air gap flux requires the use of some Hall sensors (Umanand & Bhat, 1995), which requires specially constructed induction motor. On one hand, they are very sensitive to temperature and mechanical vibrations. The flux signal is highly distorted by slot harmonics (Kreindler, 1994), whose spectrum and amplitude depend on the rotor speed (hence, the difficulty to be filtered).
The implementation of the indirect field-oriented control requires the identification of rotor flux instantaneous position, and the calculus of stator current prescribed value in sensorless vector control system (Gadue et. al. 2009; Griva et al. 1997; Lascu et al. 2004). The

transformation of stator axes and calculus of commands have to be applied to the inverter to obtain this current. The flux estimation is dependent on the induction machine parameters.
In this chapter, we present a comparison of the performances among three rotor flux observers. If the rotor flux is applied as criterion in the vector control of induction motor, the value and direction of the flux needs to be known. Starting from two induction motor mathematical models, this section analyses theoretically and in terms of simulation, the performances of a conventional rotor flux simulator with a view to the temperature influence of the rotor resistance. Flux observers were used to estimate the flux, since classic methods do not seem to provide acceptable performances. This section analyses the performances of a robust-adaptive rotor flux observer, starting from a mathematical model and using simulation.
Section 2 presents the analysis of conventional flux simulators based on the current and tension model of the induction model. The numerical simulation results of the two simulators generate conclusions regarding their implementation in applications. In section 3, we introduce the adaptive flux observer and present simulation tests of its robustness in rotor resistance variation with temperature. Closed-loop vector control system with robust-adaptive flux observer is introduced in section 4. The correct estimation methods of the rotor flux magnitude and position are checked and we verify if the system orients itself after the rotor flux direction.

2. Analysis of the conventional flux simulators

The structure of the adaptive observers is based on the combination of a simulator for the estimated magnitude with a corrector for the estimation error (Schauder, 1989). For the asynchronous motor, two types of such simulators can be inferred:
- simulator based on a current model;
- simulator based on a tension model.

2.1 Non-linear current model

An asynchronous motor model with a random orthogonal reference is going to be built to be used for flux observer and speed estimator simulation, in rotor resistance identification in sensorless vector control.
When the motor is sinusoidal voltage fed and it functions in a random reference, the equivalent classic single-phase scheme of asynchronous motor is built according to Fig. 1.

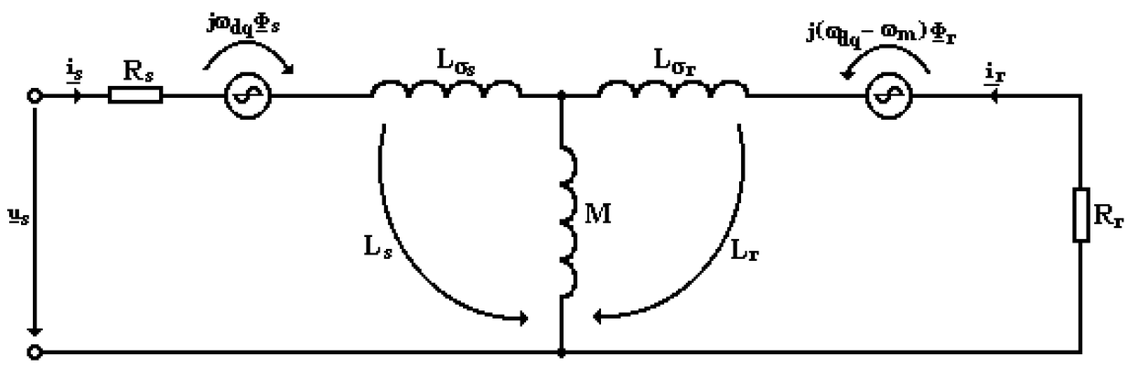

Fig. 1. Equivalent single-phase scheme of asynchronous motor in a random orthogonal reference

In a randomly oriented orthogonal reference, the vector equations of the asynchronous motor, considering d axes as the real axes (1), and q axes as the imaginary direction (j), can be written as follows:

$$\begin{cases} \underline{u}_s = R_s \cdot \underline{i}_s + \dfrac{d\underline{\Phi}_s}{dt} + j \cdot \omega_{dq} \cdot \underline{\Phi}_s \\ \underline{u}_r = 0 = R_r \cdot \underline{i}_r + \dfrac{d\underline{\Phi}_r}{dt} + j \cdot \left(\omega_{dq} - \omega_m\right) \cdot \underline{\Phi}_r \end{cases} \quad (1)$$

where:

$$\begin{cases} \underline{u}_s = u_{sd} + j \cdot u_{sq} \\ \underline{u}_r = u_{rd} + j \cdot u_{rq} \end{cases} \quad \begin{cases} \underline{i}_s = i_{sd} + j \cdot i_{sq} \\ \underline{i}_r = i_{rd} + j \cdot i_{rq} \end{cases} \quad \begin{cases} \underline{\Phi}_s = \Phi_{sd} + j \cdot \Phi_{sq} \\ \underline{\Phi}_r = \Phi_{rd} + j \cdot \Phi_{rq} \end{cases} \quad (2)$$

The expressions of stator and rotor fluxes, according to Fig. 1, can be written as follows:

$$\begin{cases} \Phi_{sd} = L_s \cdot i_{sd} + M \cdot i_{rd} \\ \Phi_{sq} = L_s \cdot i_{sq} + M \cdot i_{rq} \end{cases} \quad \begin{cases} \Phi_{rd} = L_s \cdot i_{rd} + M \cdot i_{sd} \\ \Phi_{rq} = L_s \cdot i_{rq} + M \cdot i_{sq} \end{cases} \quad (3)$$

The non-linear model of the asynchronous motor has as input data the stator orthogonal voltages that resulted from the three-phased voltages by means of a Park system transform [*P(0)*], and as output data, the stator currents and the rotor fluxes in the two orthogonal axes.
The expressions of rotor currents are obtained from relations (3), according to model input values:

$$\begin{cases} i_{rd} = \dfrac{1}{L_r}(\Phi_{rd} - M \cdot i_{sd}) \\ i_{rq} = \dfrac{1}{L_r}(\Phi_{rq} - M \cdot i_{sq}) \end{cases} \quad (4)$$

The derived rotor flux expressions are obtained from rotor voltage equations (1):

$$\begin{cases} \dfrac{d\Phi_{rd}}{dt} = -R_r \cdot i_{rd} + (\omega_{dq} - \omega_m) \cdot \Phi_{rq} \\ \dfrac{d\Phi_{rq}}{dt} = -R_r \cdot i_{rq} - (\omega_{dq} - \omega_m) \cdot \Phi_{rd} \end{cases} \quad (5)$$

Relations (4) and (5) are replaced and the expressions of two model output are obtained according to the model input:

$$\begin{cases} \dfrac{d\Phi_{rd}}{dt} = \dfrac{R_r \cdot M}{L_r} \cdot i_{sd} - \dfrac{R_r}{L_r} \cdot \Phi_{rd} + (\omega_{dq} - \omega_m) \cdot \Phi_{rq} \\ \dfrac{d\Phi_{rq}}{dt} = \dfrac{R_r \cdot M}{L_r} \cdot i_{sq} - \dfrac{R_r}{L_r} \cdot \Phi_{rq} - (\omega_{dq} - \omega_m) \cdot \Phi_{rd} \end{cases} \quad (6)$$

The stator flux expressions (3) of the two orthogonal axes are replaced in the stator voltage equations (1) and there results:

$$\begin{cases} \dfrac{di_{sd}}{dt} = \dfrac{1}{L_s}(-M\dfrac{di_{rd}}{dt} - R_s \cdot i_{sd} + \omega_{dq} \cdot L_s \cdot i_{sq} + \omega_{dq} \cdot M \cdot i_{rq} + u_{sd}) \\ \dfrac{di_{sq}}{dt} = \dfrac{1}{L_s}(-M\dfrac{di_{rq}}{dt} - R_s \cdot i_{sq} - \omega_{dq} \cdot L_s \cdot i_{sd} - \omega_{dq} \cdot M \cdot i_{rd} + u_{sq}) \end{cases} \tag{7}$$

The rotor current expressions obtained in (4) are replaced, and then, the relations (6) are replaced in (7) and we obtain:

$$\begin{cases} \dfrac{di_{sd}}{dt} = \dfrac{1}{1-\dfrac{M^2}{L_s L_r}}\left\{-(\dfrac{R_s}{L_s} + \dfrac{R_r M^2}{L_s L_r{}^2}) \cdot i_{sd} + (1-\dfrac{M^2}{L_s L_r})\omega_{dq} \cdot i_{sq} + \dfrac{R_r M}{L_s L_r{}^2} \cdot \Phi_{rd} + \dfrac{M}{L_s L_r}\omega_m \cdot \Phi_{rq}\right\} \\ \dfrac{di_{sd}}{dt} = \dfrac{1}{1-\dfrac{M^2}{L_s L_r}}\left\{-(1-\dfrac{M^2}{L_s L_r})\omega_{dq} \cdot i_{sd} - (\dfrac{R_s}{L_s} + \dfrac{R_r M^2}{L_s L_r{}^2}) \cdot i_{sq} - \dfrac{M}{L_s L_r}\omega_m \cdot \Phi_{rd} + \dfrac{R_r M}{L_s L_r{}^2} \cdot \Phi_{rq}\right\} \end{cases} \tag{8}$$

The total dispersion coefficient is defined noted by:

$$\sigma = 1 - \frac{M^2}{L_s L_r}, \tag{9}$$

value which simplifies considerably the writing of the equations characterizing the non-linear model:
Relations (8) noted with (9) become:

$$\begin{cases} \dfrac{di_{sd}}{dt} = -(\dfrac{R_s}{\sigma L_s} + \dfrac{R_r(1-\sigma)}{\sigma L_r}) \cdot i_{sd} + \omega_{dq} \cdot i_{sq} + \dfrac{R_r(1-\sigma)}{\sigma M L_r} \cdot \Phi_{rd} + \dfrac{1-\sigma}{\sigma M} \cdot \omega_m \cdot \Phi_{rq} \\ \dfrac{di_{sd}}{dt} = -\omega_{dq} \cdot i_{sd} - (\dfrac{R_s}{\sigma L_s} + \dfrac{R_r(1-\sigma)}{\sigma L_r}) \cdot i_{sq} - \dfrac{1-\sigma}{\sigma M} \cdot \omega_m \cdot \Phi_{rd} + \dfrac{R_r(1-\sigma)}{\sigma M L_r} \cdot \Phi_{rq} \end{cases} \tag{10}$$

Differential equations (6) and (10) describe a system of "electrical" differential equations which can be expresses as a state vector system:

$$\begin{cases} \dfrac{d}{dt}X_e = A_e \cdot X_e + B_e \cdot U_e \\ Y_e = C_e \cdot X_e \end{cases} \tag{11}$$

where:

- state vector is:

$$X_e = \begin{bmatrix} i_{sd} & i_{sq} & \Phi_{rd} & \Phi_{rq} \end{bmatrix}^T \tag{12}$$

- excitation vector is:

$$U_e = \begin{bmatrix} u_{sd} \\ u_{sq} \end{bmatrix} \tag{13}$$

- state matrix is:

$$A_e = \begin{bmatrix} -(\frac{R_s}{\sigma L_s} + \frac{R_r(1-\sigma)}{\sigma L_r}) & \omega_{dq} & \frac{R_r(1-\sigma)}{\sigma M L_r} & \frac{1-\sigma}{\sigma M}\cdot\omega_m \\ -\omega_{dq} & -(\frac{R_s}{\sigma L_s} + \frac{R_r(1-\sigma)}{\sigma L_r}) & -\frac{1-\sigma}{\sigma M}\cdot\omega_m & \frac{R_r(1-\sigma)}{\sigma M L_r} \\ \frac{MR_r}{L_r} & 0 & -\frac{R_r}{L_r} & \omega_{dq}-\omega_m \\ 0 & \frac{MR_r}{L_r} & -(\omega_{dq}-\omega_m) & -\frac{R_r}{L_r} \end{bmatrix} \quad (14)$$

- state matrix, vector and matrix of initial conditions are:

$$B_e = \begin{bmatrix} \frac{1}{\sigma L_s} & 0 \\ 0 & \frac{1}{\sigma L_s} \\ 0 & 0 \\ 0 & 0 \end{bmatrix}$$

$$Y_e = \begin{bmatrix} i_{sd} \\ i_{sq} \end{bmatrix} \qquad C_e = \begin{bmatrix} 1 & 0 & 0 & 0 \\ 0 & 1 & 0 & 0 \end{bmatrix} \quad (15)$$

A more simplified form can be used with respect to the notations if stator and rotor time constants are noted with:

$$\tau_s = \frac{L_s}{R_s} \qquad \tau_r = \frac{L_r}{R_r}. \quad (16)$$

A state matrix becomes:

$$A = \begin{bmatrix} -(\frac{1}{\sigma\tau_s} + \frac{1-\sigma}{\sigma\tau_r}) & \omega_{dq} & \frac{1-\sigma}{\sigma M\tau_r} & \frac{1-\sigma}{\sigma M}\cdot\omega_m \\ -\omega_{dq} & -(\frac{1}{\sigma\tau_s} + \frac{1-\sigma}{\sigma\tau_r}) & -\frac{1-\sigma}{\sigma M}\cdot\omega_m & \frac{1-\sigma}{\sigma M\tau_r} \\ \frac{M}{T_r} & 0 & -\frac{1}{\tau_r} & \omega_{dq}-\omega_m \\ 0 & \frac{M}{\tau_r} & -(\omega_{dq}-\omega_m) & -\frac{1}{\tau_r} \end{bmatrix} \quad (17)$$

This generalised non-linear model of the induction motor applies to a random reference both in transient and permanent regimes.
In a stator related reference, (*d*-*q*) ≡ (d_s-q_s), the condition for the equation system (11) is:

$$\omega_{dq} = 0 \quad (18)$$

Under these conditions, the differential equation system is:

$$\frac{d}{dt}\begin{bmatrix} i_{sd} \\ i_{sq} \\ \Phi_{sd} \\ \Phi_{sq} \end{bmatrix} = \begin{bmatrix} -(\frac{1}{\sigma\tau_s}+\frac{1-\sigma}{\sigma\tau_r}) & 0 & \frac{1-\sigma}{\sigma M\tau_r} & \frac{1-\sigma}{\sigma M}\cdot\omega_m \\ 0 & -(\frac{1}{\sigma\tau_s}+\frac{1-\sigma}{\sigma\tau_r}) & -\frac{1-\sigma}{\sigma M}\cdot\omega_m & \frac{1-\sigma}{\sigma M\tau_r} \\ \frac{M}{\tau_r} & 0 & -\frac{1}{\tau_r} & -\omega_m \\ 0 & \frac{M}{\tau_r} & \omega_m & -\frac{1}{\tau_r} \end{bmatrix} \cdot \begin{bmatrix} i_{sd} \\ i_{sq} \\ \Phi_{sd} \\ \Phi_{sq} \end{bmatrix} + \begin{bmatrix} \frac{1}{\sigma L_s} & 0 \\ \frac{1}{\sigma L_s} & 0 \\ 0 & 0 \\ 0 & 0 \end{bmatrix} \cdot \begin{bmatrix} u_{sd} \\ u_{sq} \end{bmatrix} \tag{19}$$

To this "electrical" differential equation system we add a "mechanical" equation system (*m* indices) which can be written as:

$$\begin{cases} \frac{d}{dt}X_m = A_m \cdot X_m + B_m \cdot U_m \\ Y_m = C_m \cdot X_m \end{cases} \tag{20}$$

where,

$$X_m = \begin{bmatrix} \omega_m \\ m_{rez} \end{bmatrix} \qquad A_m = \begin{bmatrix} -\frac{F_f}{J} & -\frac{p}{J} \\ 0 & 0 \end{bmatrix} \qquad U_m = m_e \tag{21}$$

and

$$B_m = \begin{bmatrix} \frac{p}{J} \\ 0 \end{bmatrix} \qquad C_m = \begin{bmatrix} 1 & 0 \\ 0 & 0 \end{bmatrix} \tag{22}$$

The expression of the electromagnetic torque which is expressed according to model output values is:

$$m_e = \frac{3}{2}\cdot p \cdot \frac{M}{L_r}\cdot(\Phi_{rd}\cdot i_{sq} - \Phi_{rq}\cdot i_{sd}) \tag{23}$$

Relations (19), (20) and (23) underlay the achievement of current non-linear model of asynchronous motor **(I_mas_md)** that was used in all estimators and identification algorithms of induction motor parameters.

2.2 Voltage non-linear model

This model has two orthogonal axes and load torque as input values, and stator and rotor currents between the two axes as output values.

For a random reference *d-q*, the derivative expressions in relation with the rotor current times are calculated on the basis of the general relations (1), (3), thus resulting the following differential "electrical" system, expressed by means of state vectors:

$$\begin{cases} \dfrac{d}{dt} X_e = A_e \cdot X_e + B_e \cdot U_e \\ Y_e = C_e \cdot X_e \end{cases} \tag{24}$$

where:

- state vector is:

$$X_e = \begin{bmatrix} i_{sd} & i_{sq} & i_{rd} & i_{rq} \end{bmatrix}^{tT} \tag{25}$$

- excitation vector is:

$$U_e = \begin{bmatrix} u_{sd} \\ u_{sq} \end{bmatrix} \tag{26}$$

- state matrix is:

$$A_e = \begin{bmatrix} -\dfrac{R_s}{\sigma L_s} & -\dfrac{(\omega_{dq}-\omega_m)\cdot M^2}{\sigma L_s L_r} + \dfrac{\omega_{dq}}{\sigma} & \dfrac{R_r M}{\sigma L_s L_r} & \dfrac{M}{\sigma L_s}\cdot\omega_m \\ \dfrac{(\omega_{dq}-\omega_m)\cdot M^2}{\sigma L_s L_r} - \dfrac{\omega_{dq}}{\sigma} & -\dfrac{R_s}{\sigma L_s} & -\dfrac{M}{\sigma L_s}\omega_m & \dfrac{R_r M}{\sigma L_s L_r} \\ \dfrac{R_s}{\sigma L_s} & -\omega_m \dfrac{M}{\sigma L_r} & -\dfrac{R_r}{\sigma L_r} & \dfrac{\omega_{dq}-\omega_m}{\sigma} - \dfrac{\omega_{dq} M^2}{\sigma L_s L_r} \\ \omega_m \dfrac{M}{\sigma L_r} & \dfrac{R_s}{\sigma L_s} & -\dfrac{\omega_{dq}-\omega_m}{\sigma} + \dfrac{\omega_{dq} M^2}{\sigma L_s L_r} & -\dfrac{R_r}{\sigma L_r} \end{bmatrix} \tag{27}$$

- excitation matrix, vector and matrix of the initial conditions are:

$$B_e = \begin{bmatrix} \dfrac{1}{\sigma L_s} & 0 \\ 0 & \dfrac{1}{\sigma L_s} \\ -\dfrac{M}{\sigma L_s L_r} & 0 \\ 0 & -\dfrac{M}{\sigma L_s L_r} \end{bmatrix} \quad Y_e = \begin{bmatrix} i_{sd} \\ i_{sq} \end{bmatrix} \quad C_e = \begin{bmatrix} 1 & 0 & 0 & 0 \\ 0 & 1 & 0 & 0 \end{bmatrix} \tag{28}$$

To this differential system we add the "mechanical" state equations system (20), forming together voltage model **V_mas_md**.

2.3 Simulator based on the current model

Next, it will be demonstrated why the simulators cannot be used as flux observers, solution which will lead to the corrector's removal from the adaptive calculus methods. The matrix state equations describing the working of an induction motor, in orthogonal co-ordinates *d-q*

(Filote & Graur,1998; Filote et al. 2007, 2009; Marchensoni et al. 1994; Pană, 1995; Schauder, 1989), can be written in complex as:

$$\begin{bmatrix} \dot{\underline{i}}_s \\ \dot{\underline{\Phi}}_r \end{bmatrix} = \begin{bmatrix} a_{11} & a_{12} \\ a_{21} & a_{22} \end{bmatrix} \cdot \begin{bmatrix} \underline{i}_s \\ \underline{\Phi}_r \end{bmatrix} + \begin{bmatrix} b_1 \\ 0 \end{bmatrix} \cdot \begin{bmatrix} \underline{u}_s \end{bmatrix} \tag{29}$$

where:

$$\begin{cases} a_{11} = -\dfrac{R_s}{\sigma L_s} - \dfrac{R_r(1-\sigma)}{\sigma L_r}; \\ a_{12} = \dfrac{M}{\sigma L_s L_r} \cdot \left(\dfrac{R_r}{L_r} - j\omega_m \right); \end{cases} \quad \begin{cases} a_{21} = \dfrac{MR_r}{L_r} \\ a_{22} = -\dfrac{R_r}{L_r} + j\omega_m \end{cases} \quad \begin{cases} b_1 = \dfrac{MR_r}{L_r} \\ \sigma = 1 - \left(\dfrac{M^2}{L_s L_r} \right) \end{cases} \tag{30}$$

The current model can be obtained if we consider the second equation from relation (29) that allows us to touch the estimated flux as:

$$\dot{\hat{\underline{\Phi}}}_r = a_{21} \cdot \underline{i}_s + a_{22} \cdot \hat{\underline{\Phi}}_r = \left(\frac{MR_r}{L_r} \right) \cdot \underline{i}_s + \left(-\frac{R_r}{L_r} + j\omega_m \right) \cdot \hat{\underline{\Phi}}_r \tag{31}$$

The estimation error is given by the difference between the value of the estimated flux and the real one:

$$\underline{\varepsilon} = \hat{\underline{\Phi}}_r - \underline{\Phi}_r \,. \tag{32}$$

When the motor parameters are constant, the derivative of that error, which localizes the poles of the observer in complex plane, becomes:

$$\dot{\underline{\varepsilon}} = a_{22} \cdot \underline{\varepsilon} = \left(-\frac{R_r}{L_r} \pm j\omega_m \right) \cdot \underline{\varepsilon} \,. \tag{33}$$

The relation (33) shows that the derivative of the estimation error depends only by motor variable parameters (rotor resistance and inductance, motor speed), so it can be controlled. Because the poles in complex plane depend on the motor speed, the observer stability will decrease while the speed increases.

2.4 Simulator based on the tension model

The expression of the tension model can be obtained from the current model of the induction motor (29), written as follows:

$$\begin{cases} \dot{\underline{i}}_s = a_{11} \cdot \underline{i}_s + a_{12} \cdot \underline{\Phi}_r + b_1 \cdot u_s \\ \dot{\underline{\Phi}}_r = a_{21} \cdot \underline{i}_s + a_{22} \cdot \underline{\Phi}_r \end{cases} \tag{34}$$

If we replace the expression for the rotor flux in the first equation, from the relation (34), with that obtained from the second equation, there results the simulator based on the tension model, defined with the expression:

$$\underline{\hat{\dot{\Phi}}}_r = \left(a_{21} - \frac{a_{22} \cdot a_{11}}{a_{12}} \right) \cdot \underline{i}_s + \frac{a_{22}}{a_{12}} \cdot \underline{\dot{i}}_s - \frac{a_{22} \cdot b_1}{a_{12}} \cdot \underline{u}_s = \frac{L_r}{M} \cdot \left(\underline{u}_s - R_s \cdot \underline{i}_s \right) - \left(\sigma \cdot \frac{L_r L_s}{M} \right) \cdot \underline{\dot{i}}_s \tag{35}$$

In that case, the derivative of the estimation error is:

$$\dot{\varepsilon} = 0 \,. \tag{36}$$

Therefore, the simulator based on tension model is a pure integrator. Because of this reason, the simulator based on model tension does not allow reducing the initial estimation error and, at the same time, it is very sensitive at low speeds.
The advantage that the estimation error variation does not depend on R_r results in the fact that the simulator is totally insensitive to the variation of rotor resistance. Consequently, the observations made above do not have to be taken into account.

2.5 Results of numerical simulator simulations

Next, the dependence of the rotor fluxes by the variation of the rotor resistance with the temperature, at the output of a conventional simulator based on the current model of the induction motor, will be presented.
As it is well known, the rotor resistance grows up with the temperature (Leonhard, 1990) and, because of this, the results obtained for a variation with +25% will be shown.
Analyzing the dependence between the orthogonal components, the rotor flux module and the rotor resistance variation with temperature in transitory starting conditions (low speeds), the following conclusions can be inferred:

- the rotor flux doesn't remain constant with the rotor resistance variation by temperature;
- that variation concerns only the magnitude of both orthogonal components and the module of the rotor flux (Figures 2 and 3);

Consequently, that model of the induction motor cannot be used as a flux observer into a pretentious vector control system as it is the orientation system after the rotor flux.

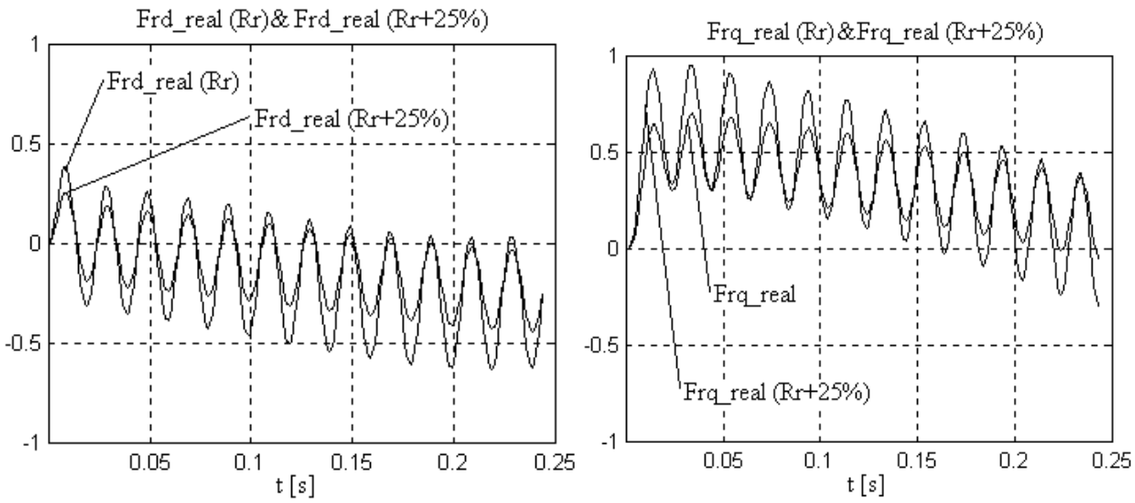

Fig. 2. Evolution of the flux orthogonal components with rotor resistance variation (low speeds).

It can be concluded that none of these simulators can be used with satisfactory results in rotor flux estimation for the asynchronous motor because of:

- the sensibility of the performances at rotor's resistance variation, for the simulator based on a current model (Fig. 2);
- the unsatisfactory low speeds working, for the simulator based on the tension model;

The satisfactory solution for indirect determination of the rotor flux is that of a robust-adaptive flux observer. Such an observer (Bose, 2006; Vas, 1998) offers remarkable robustness, with respect to the variation of the rotor's resistance, even for high values.

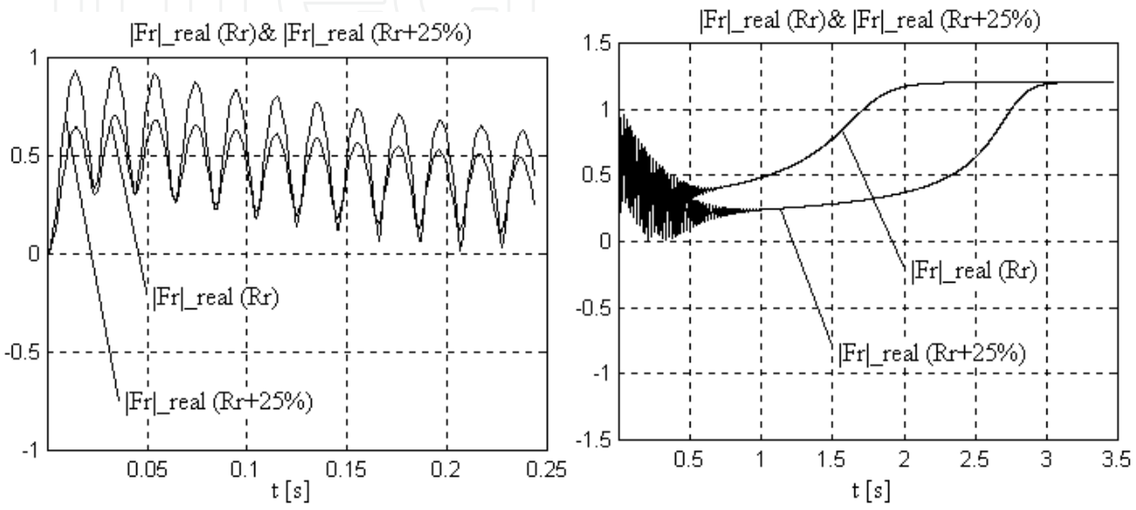

Fig. 3. Evolution of the rotor flux module due to the growth of the rotor resistance at low and high speeds.

3. Rotor flux observer

The above-mentioned disadvantages can be eliminated if flux observers are used. The latter can calculate the phasor of the rotor flux (amplitude and orientation) on the basis of some electrical units (u_s tensions and i_s stator currents) and mechanical ones (ω_m motor speed).

3.1 The structure of the flux observer

The structure of adaptive flux observers can be deduced from the linear model of induction motor (constant rotor speed) which is represented in a *d-q* system of axes, fixed on the stator and having a complex written form. This way of presentation is preferred because the study of the stability of these observers and the on-line determination of the parameters of the "matrix gate" require the fixation of the position of the poles in the complex plane.

The basic structure (Filote & Graur, 1998; Kubota et al. 1993; Pană, 1995; Schauder, 1989) of the adaptive observers consists of two essential functional elements:

- a simulator which emulates estimated values in a reference system;
- a corrector of estimated values based on an adjustable model, which is in fact a reaction loop which uses a gate to amplify, the error between the estimated value and the real one.

$$\hat{\dot{\Phi}}_r = simulator + gate * (reaction\ value - estimated\ corrector\ value) \quad (37)$$

In the case of asynchronous motor, there are two possible simulators, mainly based on:
- Current model;
- Voltage model.

These simulators, taken separately, can use two types of correctors:
- Stator equations;
- Motor voltage model.

For each corrector type, we can use three types of reaction signals:
- Stator voltage;
- Stator current;
- Stator current derivative.

Combining the above presented types of simulators, correctors and reaction signals leads us to physically achievable observer structures (Pană, 1995).
In Fig. 4, it is presented the GOPINATH type flux observer which is formed of:
- **Simulator** (reference model) based on the current model of asynchronous motor;
- **Corrector** (adjustable model) based on motor stator equation
- **Model reaction value** is stator current derivative (di_s/dt), which is obtained from the corrector
- **Gate** (auto-tuning) noted with g complex value.

From a mathematical point of view, this structure of the Gopinath flux observer can be represented as relation (37).

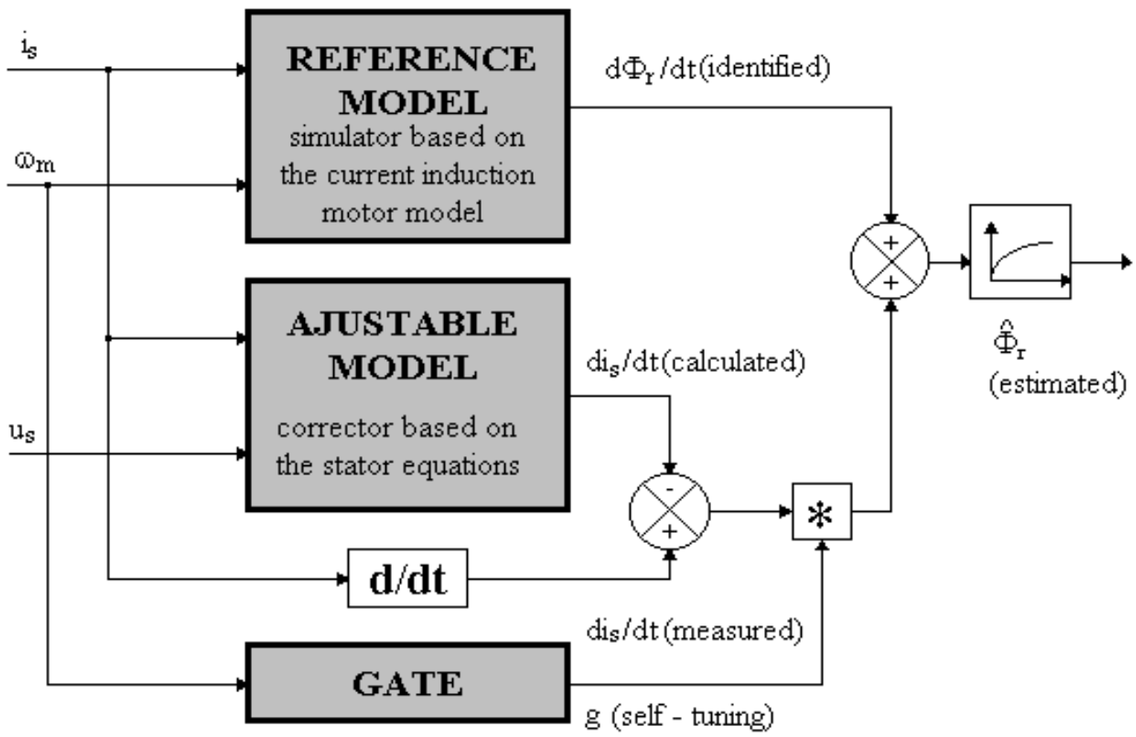

Fig. 4. The structure of the adaptive flux observer

Following the relation (37) and in accordance with Figure 4, we can obtain the **mathematical model of the estimator** (38):

$$\begin{aligned}\hat{\underline{\Phi}}_r &= a_{21}\cdot \underline{i}_s + a_{22}\cdot \hat{\underline{\Phi}}_r + \underline{g}\cdot\left[\dot{\underline{i}}_s - \left(a_{11}\cdot \underline{i}_s + a_{12}\cdot \hat{\underline{\Phi}}_r + b_1\cdot \underline{u}_s\right)\right] = \\ &= \left(a_{22} - \underline{g}\cdot a_{12}\right)\cdot \hat{\underline{\Phi}}_r + \left(a_{21} - \underline{g}\cdot a_{11}\right)\cdot \underline{i}_s - \underline{g}\cdot b_1\cdot \underline{u}_s + \underline{g}\cdot \dot{\underline{i}}_s\end{aligned} \tag{38}$$

3.2 The stability analysis

The essential element, which determines the stability of the flux observer, as well as its insensitivity to the motor parameters variation, is gate "g", a complex number:

$$g = g_a + jg_b \tag{39}$$

When motor parameters are constant, we define the estimation error, expressed by the difference between the estimated and the real rotor flux:

$$\underline{\varepsilon} = \hat{\underline{\Phi}}_r - \underline{\Phi}_r \tag{40}$$

Dynamics of estimation error (system stability) is given by the first derivative of estimation error:

$$\dot{\varepsilon} = \left(a_{22} - g\cdot a_{12}\right)\cdot \varepsilon = -h\cdot \varepsilon\ . \tag{41}$$

Relation (41) provides the position of the two complex joined poles of flux estimator; their coordinates are *Re(-h)* şi *+/-Im(-h).* As it can be noticed, the position of these two poles depends on rotor speed, by means of a_{22} şi a_{12} coefficients (relation 30).

According to stability criteria, the system is stable if and only if the poles are in the negative complex semi plane. Here, for each value of rotor speed we have to determine g_a şi g_b estimator gate coefficients, such as the two poles fulfil the stability condition. Performing the calculus in relation (41), we obtain:

$$-\frac{R_r}{L_r} + j\cdot\omega_m - \frac{M}{\sigma L_s L_r}\cdot\left(g_a + jg_b\right)\cdot\left(\frac{R_r}{L_r} - j\omega_m\right) = -\alpha + j\beta \tag{42}$$

where α and β represent the coordinates imposed to the two observer poles. Balancing the real and imaginary parts leads to a two equation system providing gate coefficients equal to:

$$g_a = \left(\frac{\frac{R_r}{L_r}\cdot\alpha + \omega_m\beta}{\left(\frac{R_r}{L_r}\right)^2 + \omega_m{}^2} - 1\right)\cdot\frac{\sigma L_s L_r}{M} \qquad g_b = \left(\frac{\omega_m\cdot\alpha - \frac{R_r}{L_r}\cdot\beta}{\left(\frac{R_r}{L_r}\right)^2 + \omega_m{}^2}\right)\cdot\frac{\sigma L_s L_r}{M} \tag{43}$$

The best position of the two poles, α and β respectively, can be obtained from the analysis of the sensitivity of the observer to the rotor resistance variation with the temperature. In the simplest case, we can adopt the position of the poles in the negative semi plane precisely on the negative axis, which leads to the following relations:

$$\begin{cases}\alpha = k\cdot\sqrt{\left(\frac{R_r}{L_r}\right)^2 + \omega_m{}^2} & (k>0)\\ \beta = 0\end{cases} \tag{44}$$

One can notice that the values of the gate coefficients depend on the rotor speed consequently they must be calculated in real time (100-200 μs).

3.3 The mathematical model of the flux observer

Explaining the coefficients from expression (6.3.10) offers the final form of the GOPINATH flux observer model:

$$\underline{\hat{\Phi}}_r = \left(a_{22} - \underline{g}\cdot a_{12}\right)\cdot\underline{\hat{\Phi}}_r + \left(a_{21} - \underline{g}\cdot a_{11}\right)\cdot\underline{i}_s - \underline{g}\cdot b_1\cdot\underline{u}_s + \underline{g}\cdot\dot{\underline{i}}_s \tag{45}$$

$$\begin{aligned}\left(\dot{\Phi}_{rd} + j\dot{\Phi}_{rq}\right) &= \left[-\frac{R_r}{L_r} + j\omega_m - \left(g_a + jg_b\right)\cdot\frac{M}{\sigma L_s L_r}\cdot\left(\frac{R_r}{L_r} - j\omega_m\right)\right]\cdot\left(\Phi_{rd} + j\Phi_{rq}\right) + \\ &+\left[\frac{MR_r}{L_r} - \left(g_a + jg_b\right)\cdot\left(-\frac{R_s}{\sigma L_s} - \frac{R_r\left(1-\sigma\right)}{\sigma L_r}\right)\right]\cdot\left(i_{sd} + ji_{sq}\right) - \\ &-\left(g_a + jg_b\right)\cdot\frac{1}{\sigma L_s}\cdot\left(u_{sd} + ju_{sq}\right) + \left(g_a + jg_b\right)\cdot\left(\dot{i}_{sd} + j\dot{i}_{sq}\right)\end{aligned} \tag{46}$$

Generally, it is advisable that the mathematical model be tested as a matrix state equation, which can be simulated or implemented in software environments from MATLAB or SIMULINK.

Matrix form of flux observer obtained from (46) is:

$$\begin{aligned}\begin{bmatrix}\dot{\Phi}_{rd}\\ \dot{\Phi}_{rq}\end{bmatrix} &= \begin{bmatrix}\left(-\frac{R_r}{L_r} - \frac{MR_r}{\sigma L_s {L_r}^2}\cdot g_a - \frac{M\omega_m}{\sigma L_s L_r}\cdot g_b\right) & -\left(\omega_m + \frac{M\omega_m}{\sigma L_s L_r}\cdot g_a - \frac{MR_r}{\sigma L_s {L_r}^2}\cdot g_b\right)\\ \left(\omega_m + \frac{M\omega_m}{\sigma L_s L_r}\cdot g_a - \frac{MR_r}{\sigma L_s {L_r}^2}\cdot g_b\right) & \left(-\frac{R_r}{L_r} - \frac{MR_r}{\sigma L_s {L_r}^2}\cdot g_a - \frac{M\omega_m}{\sigma L_s L_r}\cdot g_b\right)\end{bmatrix}\cdot\begin{bmatrix}\Phi_{rd}\\ \Phi_{rq}\end{bmatrix} + \\ &+\begin{bmatrix}-\frac{g_a}{\sigma L_s} & \frac{g_b}{\sigma L_s} & \left(\frac{MR_r}{L_r} + \frac{R_s}{\sigma L_s}g_a + \frac{R_r\left(1-\sigma\right)}{\sigma L_s}g_a\right) & -\left(\frac{R_s}{\sigma L_s}g_b + \frac{R_r\left(1-\sigma\right)}{\sigma L_r}g_b\right) & g_a & -g_b & 0\\ -\frac{g_b}{\sigma L_s} & -\frac{g_a}{\sigma L_s} & \left(\frac{R_s}{\sigma L_s}g_b + \frac{R_r\left(1-\sigma\right)}{\sigma L_r}g_b\right) & \left(\frac{MR_r}{L_r} + \frac{R_s}{\sigma L_s}g_a + \frac{R_r\left(1-\sigma\right)}{\sigma L_r}g_a\right) & g_b & g_a & 0\end{bmatrix}\cdot\begin{bmatrix}u_{sd}\\ u_{sq}\\ i_{sd}\\ i_{sq}\\ \dot{i}_{sd}\\ \dot{i}_{sq}\\ \omega_r\end{bmatrix}\end{aligned} \tag{47}$$

3.4 Results of numerical rotor flux observer simulation

The presented model has been simulated with a SIMULINK for MATLAB, which allows the inclusion of the differential system equations (47) in a simulation scheme, as shown in Fig. 5.

In accordance with the simulation scheme in Fig. 5 the values of the orthogonal components and the estimated rotor flux modulus will be compared (Fig. 6), from the output of the adaptive flux observer, with the real ones obtained at the output of the induction motor represented by the model in current (Li et al. 2005; Zhang et al. 2006).

The success of design flux observers is determined by pole assigning. The observers' sensitivity can be adjusted using gain coefficient (*k).*

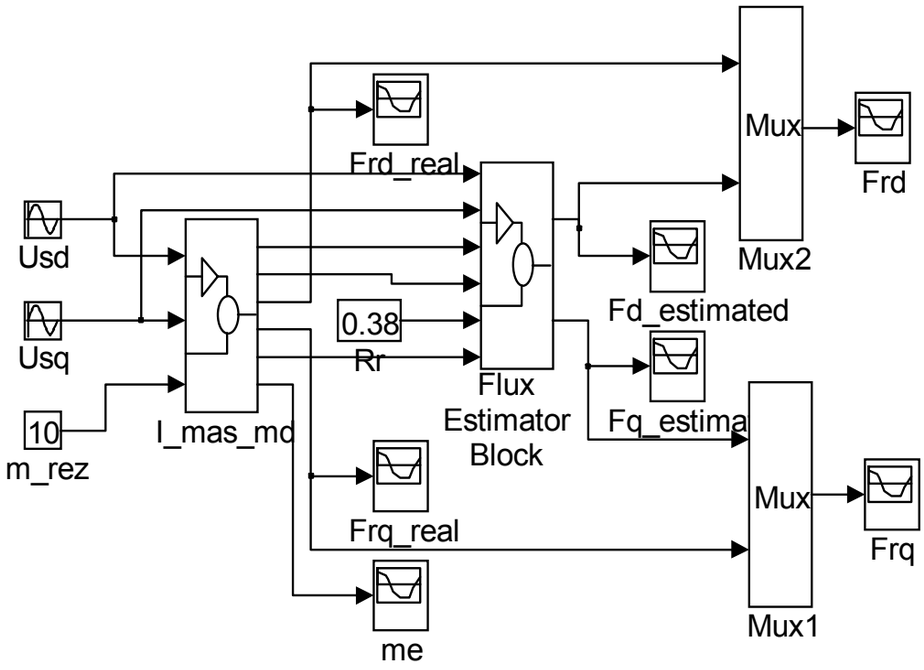

Fig. 5. The simulation scheme of the observer-motor assembly.

The very good results obtained in the flux estimation; even for important variations of the rotor, resistance with temperature (100%, in Fig. 6) demonstrates the robustness of such an observer and recommends its utilization in the applications of vector control for induction motor.

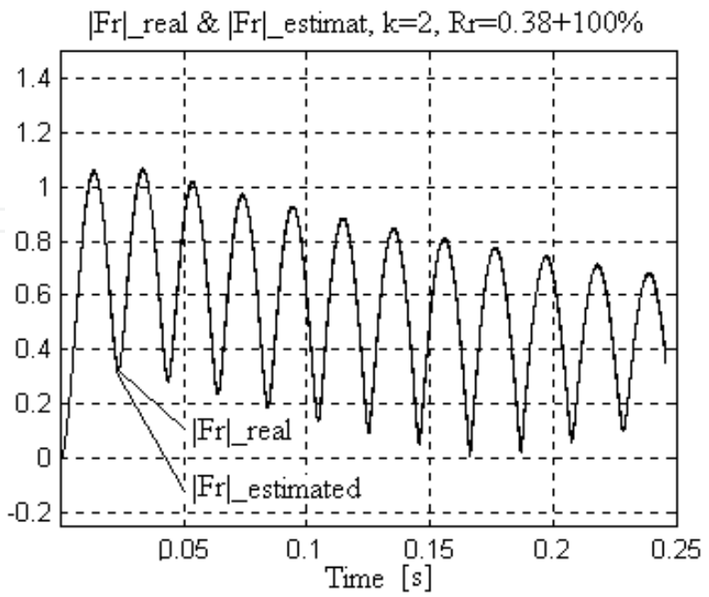

Fig. 6. Comparative presentation of the estimated (forward of the output filter) and the real rotor flux modulus.

4. Closed-loop vector control system

Figures 7 and 8 presents the bloc diagram of a rotor flux vector control system, which contains: robust-adaptive rotor flux observer, which estimates the instantaneous position and rotor flux module; vector flux analyzer that turns after rotor flux spatial vector; control algorithm and control voltage decupling block. Algorithm block is PI type and it is implemented on two control loops: closed-loop flux control and closed-loop torque control (Zhang et al. 2006).

The measured feedback values are the orthogonal components of the stator current and voltage, as well as the rotor's rotational speed. All these are applied on the robust-adaptive observer's input.

The flux analyzer calculates the modulus and the instantaneous position of the rotor flux vector, using the orthogonal components of the estimated flux. The modulus of the rotor flux and the rotor speed are feedback values in the two independent control loops of the vector control system.

The compensatory voltage block uses these two values in order to calculate the prescribed control voltage values for PWM inverter that powers the induction machine (Alexa et al. 2008; Lascu et al. 2004).

The inputs in the voltage decoupling block are the components of the stator control current, $i^*_{sd\lambda r}$ and $i^*_{sq\lambda r}$ which are provided by the two **PI** controls. The fitting of the transfer functions of the two PI controls in speed and flux is based on the relations obtained from the rotor flux orientation strategy for the reactive component $i^*_{sd\lambda r}$ and from the expression of the electromagnetic torque for the active component of the stator current $i^*_{sq\lambda r}$.

Results of real time close-loop simulation of vector control system of robust-adaptive flux observer asynchronous motor are presented by the following wave forms.

Analysis of wave forms in Fig. 9 reveals their co-sinusoidal variation and the maintenance of the two orthogonal voltages. The maximal value stabilizes fast at a value corresponding to a ratio voltage/ frequency which is dynamically calculated for an approximate $n_N/2$ speed.

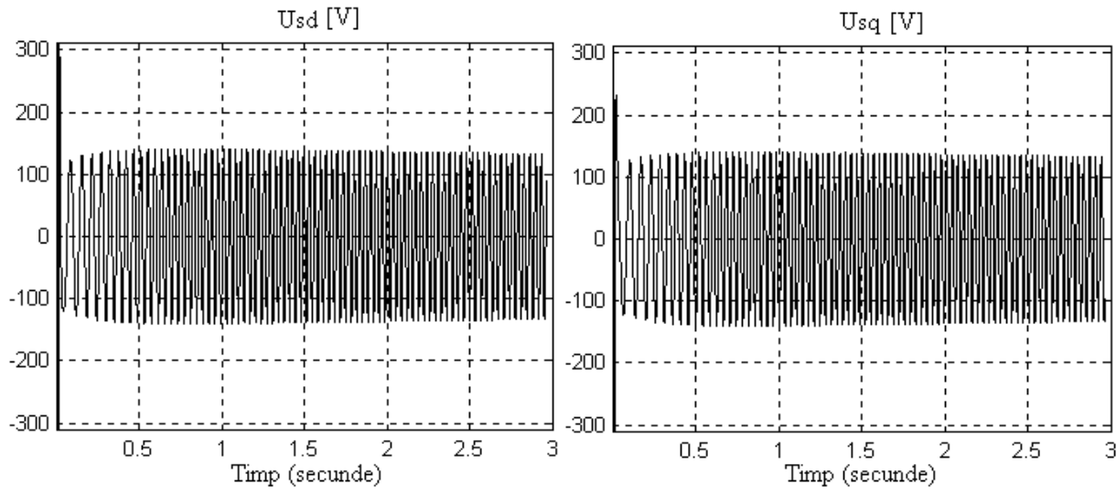

Fig. 9. Evolution of orthogonal stator voltages in a vector control system with rotor flux estimator.

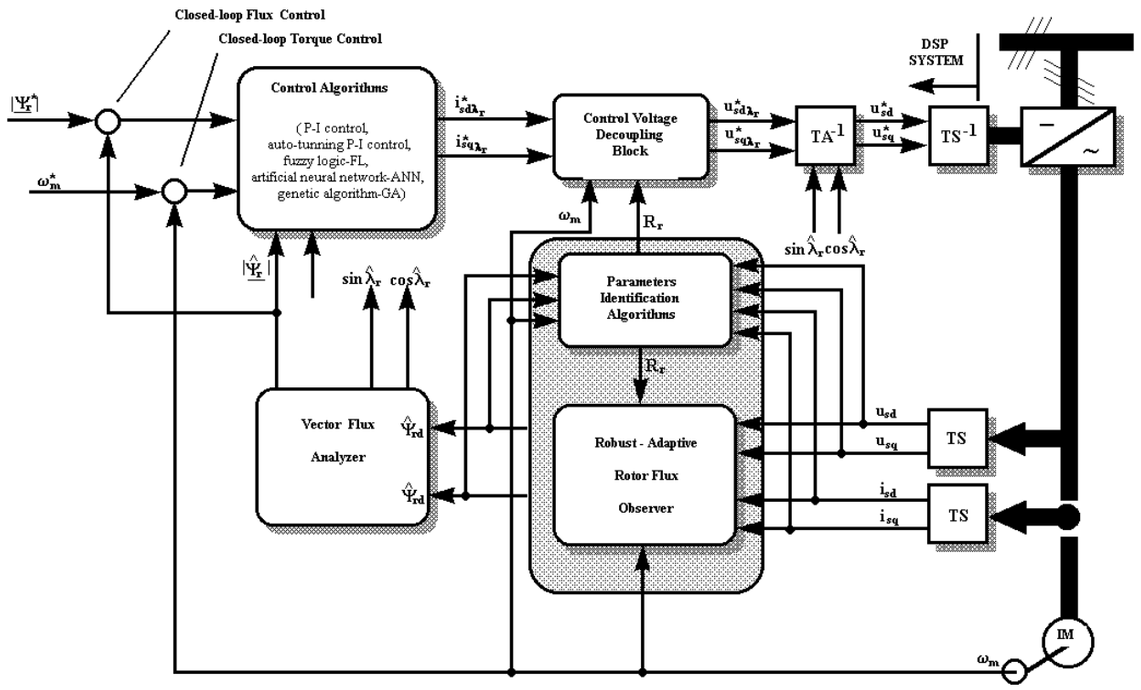

Fig. 7. Vector control of induction motor with speed rotor measurement [8].

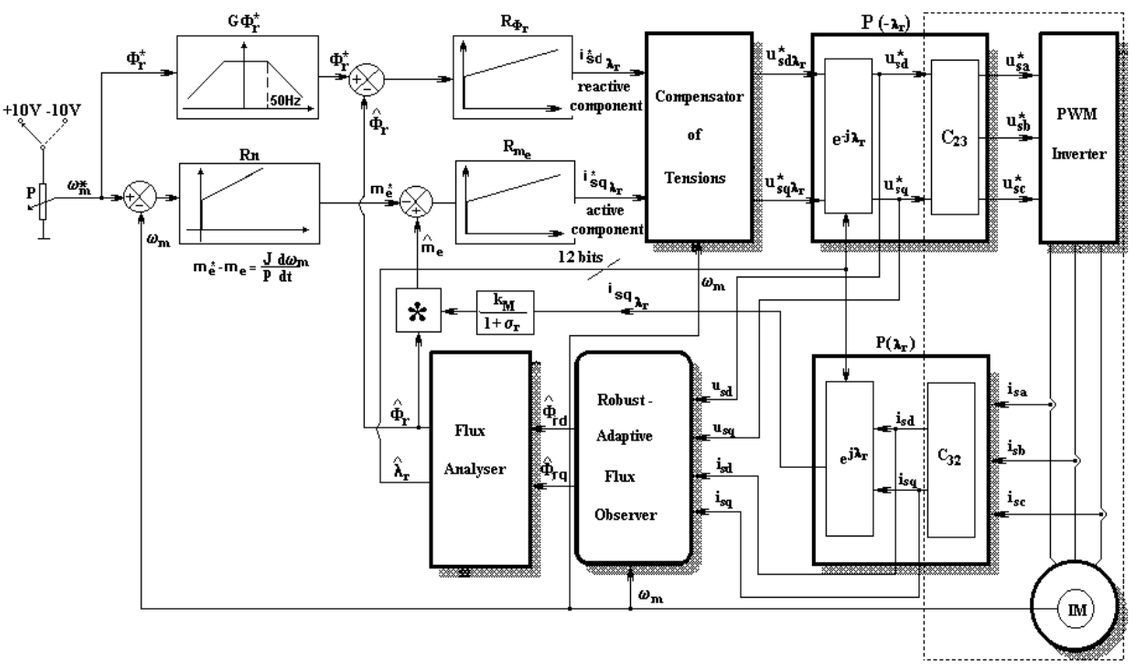

Fig. 8. Modelling of the closed-loop vector control system

The current increase in transitory regime (Fig. 10) is not as important anymore as in the case of direct start from industrial power supply, although during the simulation, the response to step signal was monitored

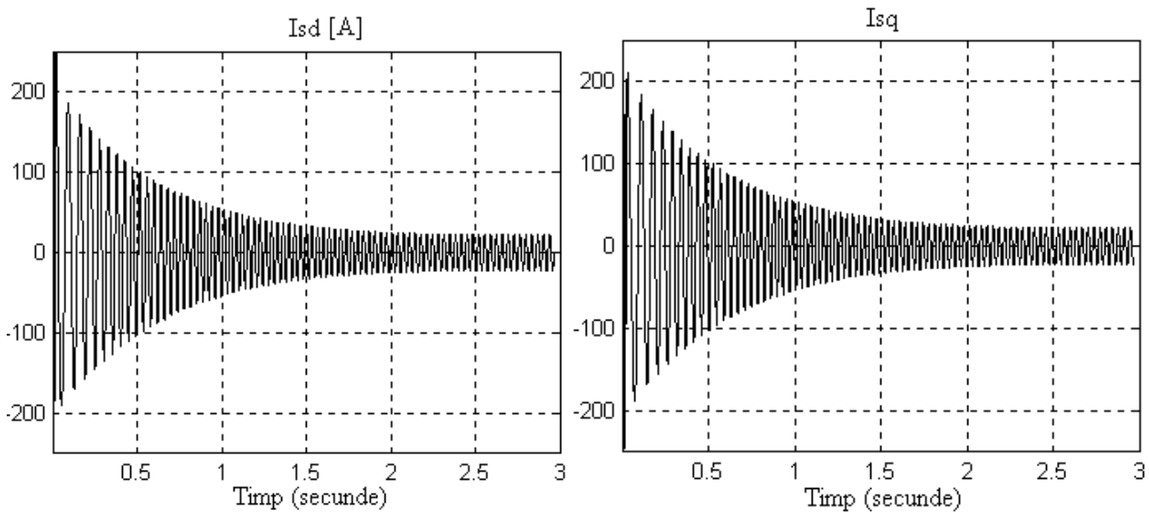

Fig. 10. The evolution of orthogonal stator currents, **a.c. values**, for vector control with robust-adaptive rotor flux estimator ($\omega_m^* = 157$ *rad/s*).

Oriented stator tensions (Fig. 11), from tension compensator output, are already d.c. values (slowly variable) after a very short time (0.01 - 0.02 s).

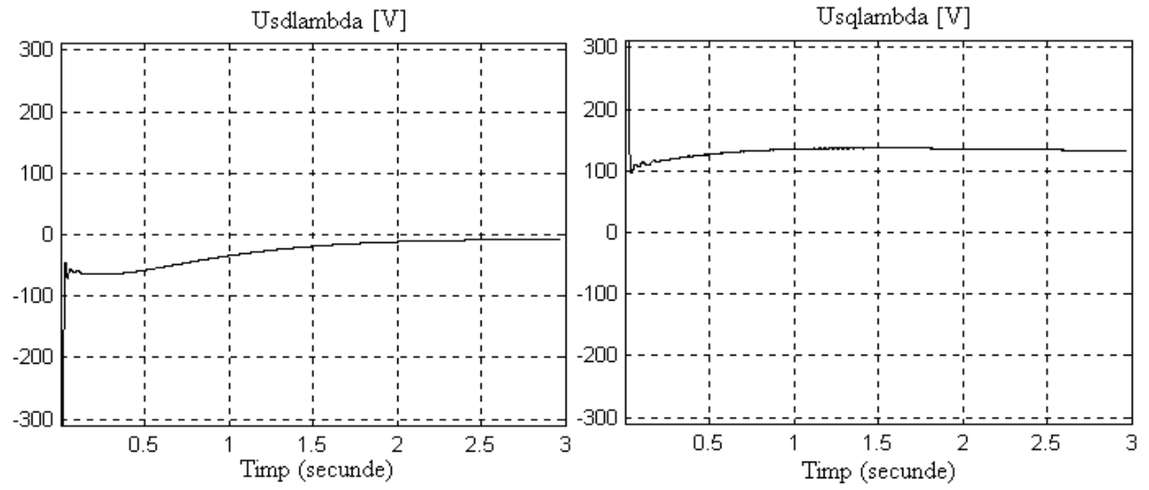

Fig. 11. The evolution of oriented orthogonal stator tensions (**d.c. values**), for vector control with robust-adaptive rotor flux estimator ($\omega_m^* = 157$ *rad/s*).

Same observation can be made for the evolution of oriented control stator currents (Fig. 12) from the output of torque and flux regulators.
The response to step signal leads to obtaining the flux (Fig. 13a) and speed (Fig. 13a) prescribed values, after the transitory regime ends. Adjusting the two regulators can be improved, thus obtaining a better indicial response.

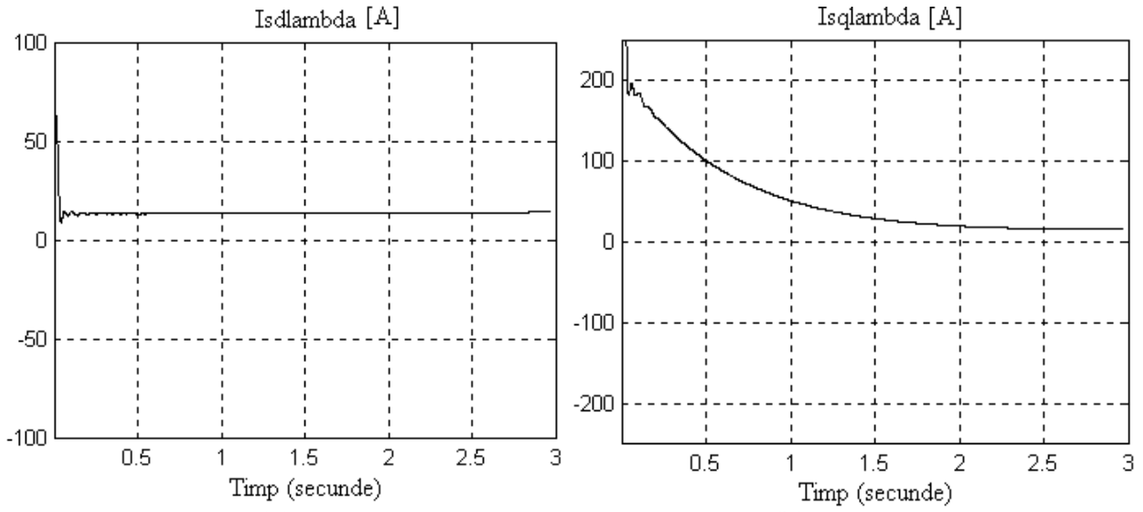

(a) (b)

Fig. 12. The evolution of oriented orthogonal stator currents (d.c. values), for vector control with robust-adaptive rotor flux estimator ($\omega_m^* = 157\ rad/s$).

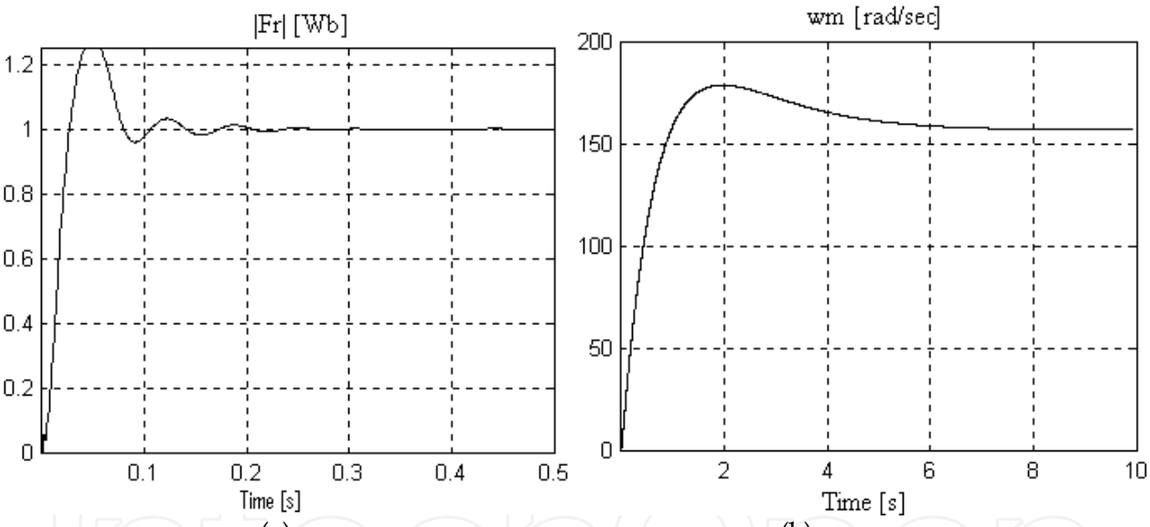

(a) (b)

Fig. 13. The evolution of rotor speed (a) and rotor modulus flux (b) for a prescribed value ω_m*=157 rad/s.

5. Conclusion

The vector control principle re-establishes the analogy with the dc motor drive. In the case of rotor flux vector control, where the control achieved by using a reference system oriented after the rotor flux direction, the two control loops of the flux and of the electromagnetic torque get decoupled and do not influence each other.

In this reference system depending on the rotor flux, the control strategy for induction motor becomes identical with the one used for the dc motor drive. Consequently, the flux becomes stable by means of the reactive component of the stator current ($i_{sd\lambda}$) and the torque by means of its active component ($i_{sq\lambda}$).

On the orientation direction after the rotor flux, the orthogonal oriented reactive stator current component ($i_{sd\lambda}$) is similar to the excitation current of dc motor drive. If we perform the calculation on λ_r direction, we obtain the following value for $i_{sd\lambda}$:

$$i_{sd\lambda} = i_{mr} = \frac{\Phi_r}{M} = \frac{1\,Wb}{0.0617\,H} \cong 16A \tag{48}$$

which is also confirmed by the results obtained during the simulation (Fig. 12a) for the orthogonal oriented reactive stator current component ($i_{sd\lambda}$). This current is similar to an excitation current i_{ex} of an dc motor drive with $\phi_{ex} = 1Wb$ and with an inductance L_{ex} equal to 61,7 mH.

$$i_{ex} = \frac{\Phi_{ex}}{L_{ex}} = \frac{1\,Wb}{0.0617\,H} \cong 16A \tag{49}$$

Before the implementation of the control algorithm on DSP systems, the simulation was the only method to prove that the system orients itself after the correct direction of the rotor flux.

6. Acknowledgements

The authors would like to acknowledge the financial support of the Romanian National Council for Project Management under Grant PN II No. 71-065 / 2007 and No. 22-137 / 2008.

7. References

Alexa, D.; Goraş, T.C. ; Sârbu, A. ; Pletea, I.V.; Filote, C. ; Ionescu, F. (2008). An Analysis of the Two-Quadrant Convertor with RNSIC, *IET Power Electronics*, Vol. 1, No. 2, (June 2008), pp. 224–234, ISSN 1755-4535

Blaabjerg, F.; Consoli, A.; Ferreira, J.A. (2005). The Future of Electronics Power Processing and Conversion, *IEEE Transactions on Industry Applications*, Vol. 41(1), 2005, pp. 3-8, ISSN 0093-9994, 2005

Bose, B. K. (2006). *Power Electronics and Motion Drives: Advances and Trends*, Elsevier, ISBN 13: 978-0-12-088405-6, USA

Bose, B. K. (2000). Energy, Environment and Advances in Power Electronics, *IEEE Transaction on Power Electronics*, Vol. 15(4), pp. 688-701, ISSN 0885-8993, 2000

Filote, C.; Graur, A. (1998). *Electrical Drives Systems. Induction machine,* Vol. 1, Editura Universităii Stefan cel Mare (Ed.), ISBN 973-98389-8-7, Suceava, Romania

Filote, C.; Alexa, D.; Pletea, I.V.; Micea, M.; Ciufudean, C.; Cozgarea, A.M. (2009). Robust-Adaptive Flux Observers in Induction Motor Drive Systems, *Proceeding of the Twelfth IASTED International Conference Intelligent Systems and Control*, ActaPress (Ed.), pp. 127-134, ISBN 978-0-88986-814-4, Cambridge, Massachusetts, USA, November 2-4, 2009

Filote, C.; Ciufudean, C.; Graur, A.; Cozgarea, A.M.; Amarandei, D.; Petrescu, C. (2008). Robust-Adaptive Flux Observer in High Performance Vector Control in Induction Motors, *International Symposium on Power Electronics, Electrical Drives, Automation*

and Motion-SPEEDAM, pp. 1097-1102, ISBN 978-1-4244-1664-6, Ischia, Italy, June 11-13, 2008

Filote, C.; Amarandei, D.; Ciufudean, C.; Graur, A.; Mandici, L. (2007). Vector Speed Control Modelling of Induction Motors Using Robust-Adaptive Flux Observer, *Proc. of The 26th IASTED International Conference Applied Simulation and Modelling – ASM 2007*, pp.479-484, ISBN 978-0-88986-687-4, Palma de Mallorca, Spain, September 1-3, 2007

Gadoue, S.M.; Giaouris, D.; Finch, J.W. (2009). Sensorless Control of Induction Motor Drives at Verry Low and Zero Speeds Using Neural Network Flux Observers, *IEEE Transations on Industrial Electronics*, Vol. 56, No. 8, pp. 3029-3039, ISSN 0278-0046, August 2009

Griva, G.; Ilas, C.; Eastham, J.F.; Profumo, F.; Vranka, P. (1997). High Performance Sensorless Control of Induction Motor Drives for Industry Applications, *Power Conversion Conference*, Vol.2, pp. 535-539, Nagaoka, Japan, 1997

Holtz, J. (2002), Sensorless Control of induction Motor Drives, Proceedings of the IEEE, Vol. 90, No. 8, pp. 1359-1394, ISSN 0018-9219, August, 2002

Kreindler, L.; Moreira, J.C.; Testa, A.; Lipo, T.A. (1994). Direct Field Orientation Controller Using the Stator Phase Voltage Thrid Harmonic, *IEEE Transaction on Industry Applications*, vol. 30, No. 2, pp. 441-447, ISSN 0093-9994, March/April, 1994

Kubota, H.; Matsuse, K.; Nakano, T. (1993). DSP-Based Speed Adaptive Flux Observer of Induction Motor, *IEEE Transactions on Industry Applications*, vol.29 , no. 2, pp. 344-348, ISSN 0093-9994, 1993

Lascu, C.; Boldea, I.; Blaabjerg, F. (2004). Direct Torque Control of Sensorless Induction Motor Drives: A Sliding-mode Appoach, *IEEE Transaction on Industrial Applications,* Vol. 40, No. 2, pp. 582-590, ISSN 0093-9994, March/April 2004.

Leonhard, W. (1990). *Control of Electrical Drives*, Springer-Verlag, ISBN 3-540-13650-9, Berlin, Germany

Li, J.; Xu, L.; Zhang, Z. (2005). An Adaptive Sliding-Mode Observer for Induction Motor Sensorless Speed Control, *IEEE Transactions on Industry Applications*, Vol. 41, No. 4, pp. 1039-1046, ISSN 0093-9994, July/August, 2005

Marchensoni, M.; Segarich, P.; Soressi, E. (1994). A Simple Approach to Flux and Speed Observation in Induction Motor Drives, *IECON*, pp. 305-310, Bologna, Italy, 1994

Schauder, C. (1989). Adaptive Speed Identification for Vector Control of Induction Motors Without Rotational Transducers, *Proc. IEEE Industry Applications Society Annual Meeting,* , pp. 493-499, San Diego, California, USA, Octomber 1-5, 1989

Pană, T. (1995). *Matlab in Electrical Drive Systems,* Universitatea Tehnica Cluj Napoca (Ed.), Romania

Umanand, L.; Bhat, S.R. (1995). On Line Estimation of the Stator Resistence of an Induction Motor for Speed Control Applications, *IEE Proceedings, Electric Power Applications*, vol.142, (March 1995), pp. 97-103, ISSN 1350-2352

Vas, P. (1998). *Sensorless vector and direct torque control,* Oxford University Press, ISBN 0-19-856465-1, Oxford, U.K.

Zhang, Z.; Xu, H.; Xu, L.; Heiman, L. (2006). Sensorless Direct Field-Oriented Control of Three-Phase Induction Motors Based on "Sliding Mode" for Washing-Machine Drive Applications, *IEEE Transaction on Industry Applications,* Vol. 42(3), pp. 694-701, ISSN 0093-9994, 2006

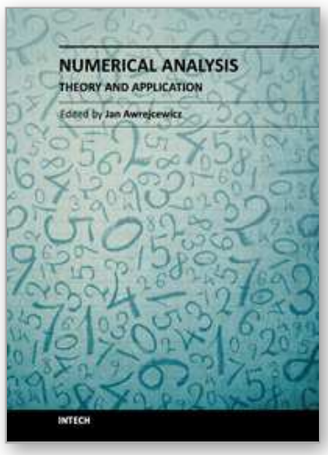

Numerical Analysis - Theory and Application

Edited by Prof. Jan Awrejcewicz

ISBN 978-953-307-389-7
Hard cover, 626 pages
Publisher InTech
Published online 09, September, 2011
Published in print edition September, 2011

Numerical Analysis â€“ Theory and Application is an edited book divided into two parts: Part I devoted to Theory, and Part II dealing with Application. The presented book is focused on introducing theoretical approaches of numerical analysis as well as applications of various numerical methods to either study or solving numerous theoretical and engineering problems. Since a large number of pure theoretical research is proposed as well as a large amount of applications oriented numerical simulation results are given, the book can be useful for both theoretical and applied research aimed on numerical simulations. In addition, in many cases the presented approaches can be applied directly either by theoreticians or engineers.

InTech Europe
University Campus STeP Ri
Slavka Krautzeka 83/A
51000 Rijeka, Croatia
Phone: +385 (51) 770 447
Fax: +385 (51) 686 166
www.intechopen.com

InTech China
Unit 405, Office Block, Hotel Equatorial Shanghai
No.65, Yan An Road (West), Shanghai, 200040, China
中国上海市延安西路65号上海国际贵都大饭店办公楼405单元
Phone: +86-21-62489820
Fax: +86-21-62489821

IntechOpen